THE ASTROPHYSICAL JOURNAL, 303:556–572, 1986 April 15

STELLAR KINEMATICS AND THE STABILITY OF DISKS IN SPIRAL GALAXIES

P. C. VAN DER KRUIT[1] AND K. C. FREEMAN
Mount Stromlo and Siding Spring Observatories, Research School of Physical Sciences, Australian National University
Received 1984 October 23; accepted 1985 July 25

ABSTRACT

We have observed the velocity dispersion of the old disk population in two spiral galaxies. In the Sc spiral NGC 5247, the radial decline of the vertical velocity dispersion $\langle V_z^2 \rangle^{1/2}$ from the center to about two disk scale lengths is consistent with that predicted for a disk of constant thickness and M/L ratio. Combined with earlier results, the $(M/L)_B$ value for the old disk is 6 ± 2 solar units ($H = 75$ km s^{-1} Mpc^{-1}) from five galaxies. The parameter $Y = V_{\rm rot}(h/M_D G)^{1/2}$, proposed by Efstathiou *et al.* as a criterion for stability against barlike modes, can now be estimated for systems with measured rotational velocity $V_{\rm rot}$ and disk scale length h (M_D is the disk mass). For eight edge-on spirals, $Y = 0.98 \pm 0.10$ (rms), and 16 inclined spirals give $Y = 1.06 \pm 0.29$. This is consistent with stability at $Y \approx 1.1$, if the old disk M/L is in the lower part of our range 6 ± 2. For the Galaxy and NGC 891, the Y values (calculated without using M/L) are 0.98 ± 0.25 and 1.07 ± 0.12. The disks then contain 25%–30% of the total mass out to the disk edge at 4–5 scale lengths.

For the Sb spiral NGC 7184, we have measured the asymmetric drift and the absorption line profile widths, which show that the radial velocity dispersion $\langle V_R^2 \rangle^{1/2}$ also decreases with radius. Our best solution has Toomre's Q rising from 1.7 to 2.2 between 0.9 and 2 scale lengths, although a constant $Q \approx 2$ is only marginally inconsistent with the data. In the inner regions, the velocity dispersion contributes significantly to the global disk stability. The observational results are similar to those of numerical simulations in realistic model galaxies.

Subject headings: galaxies: internal motions — galaxies: stellar content — galaxies: structure

I. INTRODUCTION

The stability of the disks of spiral galaxies has long been a major subject of theoretical study. Relevant parameters are only known with any certainty at all for the Galactic disk in the solar neighborhood, so that a comparison of theory and observation has been very limited indeed (e.g., Toomre, 1974). All this is in spite of the fact that gravitational instability has been a major topic as long as gravitational theory has existed. Indeed, Newton, in his correspondence with Dr. Bentley, worried about what kept the Sun and the fixed stars from collapsing together. As Jeans (1928, p. 344) himself pointed out, this was the first reference to what we now know as the Jeans instability in an infinite homogeneous medium (for a delightful discussion of Newton's thoughts on the subject and some interesting quotations, see Hoskin 1977).

It is now known that rotation is not very helpful, in that it can only stabilize low-wavenumber modes (Chandrasekhar 1961, p. 589), and that the finite thickness of disks may be relevant at small wavelengths (Goldreich and Lynden-Bell 1965). These latter authors went on and suggested that sheared gravitational instabilities in the gas layer may be the key to the problem of spiral structure (see also Toomre 1981). The stability of *stellar* disks was addressed by Toomre (1964), who showed that the stellar velocity dispersion needs to exceed a certain critical value to ensure stability of (local) axisymmetric modes. Criteria for stability against global (barlike) modes have been found empirically by Ostriker and Peebles (1973) and Efstathiou, Lake, and Negroponte (1982). A recent review has been presented by Sellwood (1983).

The basic reason why comparison to actual galaxies has been difficult or even impossible until now is of course that these criteria must contain a space or surface density. Toomre's (1964) criterion for local stability in the stellar disk, which is of course fundamental to an understanding of disk dynamics, has the added difficulty that it also requires knowledge of the stellar velocity dispersion. In this paper we address both the density distributions in stellar disks, as measured through the vertical velocity dispersion of the stars, *and* the parallel velocity dispersions that enter Toomre's criterion. We will to this end present observations of stellar kinematics in a nearly face-on spiral (NGC 5247) and a highly inclined galaxy (NGC 7184). This is a continuation of our work presented recently (van der Kruit and Freeman 1984).

II. BACKGROUND AND APPROACH

Our first concern is the vertical velocity dispersion and the mass distribution in galactic disks. Since the stellar disks are probably self-gravitating (for some numerical estimates supporting this point see van der Kruit 1983), a combination of the thickness and the velocity dispersion gives the mass surface density. At the basis of this analysis lies the description of the light distribution of the old disk population by a locally isothermal sheet, as proposed by van der Kruit and Searle (1981*a*). This implicitly assumes that the mass distribution is similar. It can be shown that the Galactic disk in the solar neighborhood is consistent with this description (van der Kruit 1983). Now it also involves the assumption that the "missing mass" in the solar neighborhood is distributed like the old disk population. This is not unreasonable, since of the luminous constituents of the local disk, the old disk population contains most of the mass. Using a z-velocity dispersion of 30 ± 5 km s^{-1}, van der Kruit (1983) finds a local surface density of $110 \pm 20\ M_\odot$ pc^{-2}. The recent compilation of Jahreiss and Wielen (1983) suggests that a more appropriate choice may be 25 ± 5 km s^{-1} from all stars older than a few Gyr; then the

[1] Also Kapteyn Astronomical Institute, University of Groningen, The Netherlands.

surface density would be $80 \pm 20\ M_\odot\ \mathrm{pc}^{-2}$. Note that this is consistent with the value of $83 \pm 8\ M_\odot\ \mathrm{pc}^{-2}$ found in the multicomponent treatment by Bahcall (1984*b*), where we note that our assumption corresponds closely to his model 14 in which the dark matter has a z-dispersion of 20 km s^{-1}. Our single-component treatment appears to be a reasonable approximation (see also below).

The distribution of the light from the old disk population then is described by

$$L(R, z) = L(0, 0) \exp(-R/h)\ \mathrm{sech}^2(z/z_0) \quad (1)$$

for $R < R_{\max}$ (van der Kruit and Searle 1981*a*). This can be related to a stellar z-velocity dispersion with

$$\langle V_z^2 \rangle_* = \pi G \sigma(R) z_0 = 2\pi G \rho(R, 0) z_0^2 , \quad (2)$$

with $\rho(R, 0) = L(R, 0)(M/L)$ and the surface density $\sigma(R) = 2z_0\, \rho(R, 0)$, where all properties refer to the old disk population. Unless specified otherwise, all parameters in this paper refer to this population. Equation (2) is a solution based on Poisson's equation in the plane-parallel case. This is an excellent approximation in galaxies with a flat rotation curve (see discussion of eq. [6]). The constancy of $(M/L)_{\text{old disk}}$ is consistent with the observed constant color index (van der Kruit and Searle 1981*b*, 1982) and has been derived for at least the interval $R = (1.7\text{–}3.0)h$ in NGC 891 (van der Kruit 1981) by comparing the thickness of the H I layer to the H I velocity dispersion in face-on systems (Shostak and van der Kruit 1984; van der Kruit and Shostak 1984).

Combining equations (1) and (2), we find the radial dependance of the vertical velocity dispersion to be

$$\langle V_z^2 \rangle_*^{1/2} = (2\pi G \rho_0)^{1/2} z_0 \exp(-R/2h) , \quad (3)$$

where $\rho_0 = L(0, 0)(M/L)$. Our first aim in this paper is to make a detailed check on this prediction. Some indication that this is indeed true comes from our earlier work (van der Kruit and Freeman 1984), where we measured stellar velocity dispersions of order 60–80 km s^{-1} in the two face-on systems NGC 628 and 1566 at about one scale length from the center. This is considerably higher than the value for the solar neighborhood (see above) at 1.5–2.0 scale lengths. Based on these two systems, NGC 891 and the solar neighborhood, a value for the $(M/L)_{\text{old disk}}$ of (5–10) $M_\odot/L_{\odot, B}$ was derived using distances based on $H = 75$ km s^{-1} Mpc^{-1}. This implies that more than half the mass within the disk radius $R_{\max}$ resides in the halos (van der Kruit 1983; van der Kruit and Searle 1982; van der Kruit and Freeman 1984; van der Kruit and Shostak 1984). This knowledge of the disk mass makes it possible to estimate the property $Y = V_{\max}(h/GM_{\text{disk}})^{1/2}$, which Efstathiou, Lake, and Negroponte (1982) suggest as a criterion for disk stability against global barlike modes. We discuss this below.

The validity of the use of equation (2) may be questioned on two grounds, namely (i) that the disk is not in reality made up of one isothermal component, and (ii) that the component in question—the old disk population—is not entirely self-gravitating in view of the presence of a substantial amount of matter outside the disk. These matters have been covered in great detail by Bahcall (1984*a*, *b*) and recently applied to external systems by Bahcall and Casertano (1984). From their Figure 1 and equation (7) it can be seen that the correction to the calculated velocity dispersion given the values for the surface density and logarithmic slope ($= 2z_0$) over the relevant range of galactocentric distance is 10% or less for $z < z_0$ in these four systems. Since essentially all light comes from this range of z, the integrated velocity dispersions in such systems when seen face-on are also 10% or less different from the ones derived directly using the simple-minded assumptions at the basis of equation (2). This difference is insignificant compared to the observational inaccuracies that present techniques allow in the measurement of stellar velocity dispersion in disks of galaxies.

There is no detailed a priori prediction on the radial dependence of $\langle V_R^2 \rangle^{1/2}$. However, as long as the epicyclic approximation remains valid we will have $\langle V_R^2 \rangle^{1/2} / \langle (V_\theta - V_t)^2 \rangle^{1/2} = [(B-A)/B]^{1/2}$, where V_t is the stellar rotation velocity, and A and B are the local Oort constants. Even the local derivatives of the stellar velocity dispersions in our Galaxy are unknown, although some evidence that these decrease with radius has been provided by Erickson (1975). The relatively sharp edges in the radial light distribution (1) at $R_{\max}$ for the old disks in edge-on galaxies shows that the parallel velocity dispersions must drop to values at most around 10–15 km s^{-1} at these radii (van der Kruit and Searle 1981*a*, 1982). Application of Toomre's (1964) criterion for local stability suggests also that a radial decline is required to maintain marginal stability (see, e.g., Mayor 1974).

In the context of the structure of the old disk population and its kinematics, the criterion of Toomre (1964) is one of fundamental importance. For a thin disk with a reasonable form of the distribution function, Toomre finds that stability for axisymmetric modes requires

$$Q = \frac{\langle V_R^2 \rangle^{1/2} \kappa}{3.36 G \sigma} > 1 , \quad (4)$$

where κ is the epicyclic frequency $\kappa = 2\{B(B-A)\}^{1/2}$. The behavior of Q with R is of great interest.

The measurement of $\langle V_R^2 \rangle^{1/2}$ is not easy. The galaxy has to be highly inclined or edge-on, and the measurement has to be done on the minor axis. Of course, away from the minor axis one measures a combination of the radial and tangential dispersion and on the major axis the tangential one only. In this case we can use the relation of their ratio to the Oort constants, which in turn can be derived from the rotation curve. A most serious problem is that one always has a path length through the disk; this means not only that contributions from various radii are present, but also that the profile is broadened as well by the varying line-of-sight component of the rotation along the path. Furthermore, in disks there are always the problems of low surface brightness and contamination by bulge and Population I stars. These last problems can be avoided by a proper choice of systems.

Of course, it is easier to measure a radial velocity, and we will therefore use a measurement of the asymmetrical drift as our prime method, and the observed line profiles as checks. Our basic equation, then, is the hydrodynamical equation applied to the symmetry plane. We will assume axial symmetry; this is almost certainly valid because our systems show no morphological sign of a bar or oval distortion. The equation then reads (e.g., Oort 1965, eq. [10])

$$-K_R = \frac{V_t^2}{R} - \langle V_R^2 \rangle \left[\frac{\partial}{\partial R} \ln \nu \langle V_R^2 \rangle + \frac{1}{R} \left\{ 1 - \frac{\langle (V_\theta - V_t)^2 \rangle}{\langle V_R^2 \rangle} \right\} + \frac{\langle V_R V_z \rangle}{\langle V_R^2 \rangle} \frac{\partial}{\partial z} \ln \nu \langle V_R V_z \rangle \right] , \quad (5)$$

where ν is the stellar density distribution, K_R the radial force,

and V_t the mean stellar tangential velocity. The last term is probably small. In our self-gravitating disk model, the two motions should be uncoupled, and $\langle V_R V_z \rangle = 0$. In case the velocity ellipsoid points toward the galactic center, Oort (1965) shows that the last term reduces to $(1/R)(1 - \langle V_z^2 \rangle / \langle V_R^2 \rangle)$ (see his eq. [38]), and this is probably the largest value this term may take. We will set the term equal to zero, however, strengthened by the following consideration. For an axially symmetrical system, Poisson's equation is (Oort, eq. [25])

$$\frac{\partial K_R}{\partial R} + \frac{K_R}{R} + \frac{\partial K_z}{\partial z} = -4\pi G\rho \, . \tag{6}$$

Now, near the plane the first two terms are equal to $2(A-B)(A+B)$. Over the regions of interest, our systems have flat rotation curves, so that $A = -B$ and the terms vanish altogether. So, *in the case of a flat rotation curve, a plane-parallel case is a very good approximation*, much better than Oort (1965) expected on the basis of a declining rotation curve and his values of A and B. (This effect can also be appreciated by consideration of eq. [3] in Bahcall 1984*a*.) Near the center we have rising rotation curves; then our description must break down. However, equation (1) continues to hold for small R in actually observed surface brightness distributions (van der Kruit and Searle 1981*a*). Below we use equation (5) in the region where the rotation curve is flat.

We will use of course $-K_R = V_{\rm rot}^2/R$ and $\langle (V_\theta - V_t)^2 \rangle / \langle V_R^2 \rangle = B/(B-A)$. Here $V_{\rm rot}$ is the circular velocity derived directly from the forcefield; for a component with zero velocity dispersion, the asymmetrical drift equals zero, and $V_t = V_{\rm rot}$. Further, the density distribution following from equation (1) with constant M/L gives $(\partial/\partial R) \ln \nu = -1/h$. We then have

$$V_{\rm rot}^2 - V_t^2 = \langle V_R^2 \rangle \left\{ \frac{R}{h} - R \frac{\partial}{\partial R} \ln \langle V_R^2 \rangle - \left[1 - \frac{B}{(B-A)} \right] \right\} . \tag{7}$$

So we will need to make an assumption for the radial dependence of $\langle V_R^2 \rangle^{1/2}$ which can be checked after application of our technique at various R. There are two assumptions that come to mind:

a) None of the various mechanisms proposed to explain the stellar age–velocity dispersion relation gives a *detailed* prediction for the ratio $\langle V_z^2 \rangle^{1/2} / \langle V_R^2 \rangle^{1/2}$, but it may very well be constant with radius. In that case we have, for R not too small,

$$\langle V_R^2 \rangle^{1/2} \propto \langle V_z^2 \rangle^{1/2} \propto \exp(-R/2h) \tag{8}$$

and

$$\frac{\partial}{\partial R} \ln \langle V_R^2 \rangle = -1/h \, .$$

Then

$$V_{\rm rot}^2 - V_t^2 = \langle V_R \rangle^2 \{ 2R/h - [1 - B/(B-A)] \} \, . \tag{9}$$

For the case of a flat rotation curve we have $A = -B = V_{\rm rot}/2R$ and $B/(B-A) = 0.5$, so

$$V_{\rm rot}^2 - V_t^2 = \langle V_R^2 \rangle (2R/h - 0.5) \, . \tag{10}$$

b) We could assume that the disk will heat until an equilibrium value of Q is attained somewhere near 2 (Sellwood and Carlberg 1984). In that case, $Q \approx$ constant, and

$$\langle V_R^2 \rangle^{1/2} \propto \nu/\kappa \propto \exp(-R/h)/[B(B-A)]^{1/2} \, . \tag{11}$$

We then have

$$\frac{\partial}{\partial R} \ln \langle V_R^2 \rangle = \frac{-2}{h} - \frac{\partial}{\partial R} \ln [B(B-A)]$$

and

$$V_{\rm rot}^2 - V_t^2 = \langle V_R^2 \rangle \times \left\{ \frac{3R}{h} + R \frac{\partial}{\partial R} \ln [B(B-A)] - \left[1 - \frac{B}{(B-A)} \right] \right\} . \tag{12}$$

Again we may evaluate this for a flat rotation curve when $\kappa = (2V_{\rm rot}/R)^{1/2}$ or $B(B-A) = V_{\rm rot}^2/R^2$. Then we see that $\langle V_R^2 \rangle^{1/2} \propto R \exp(-R/h)$, and

$$V_{\rm rot}^2 - V_t^2 = \langle V_R^2 \rangle (3R/h - 2.5) \, . \tag{13}$$

The difference between the two dependences is not very large: the terms in parentheses in equations (10) and equation (13) are equal at $R = 2h$. For the same $V_{\rm rot}$ and V_t, the ratio of the derived $\langle V_R^2 \rangle^{1/2}$ from equation (10) to that from equation (13) varies from 1.12 at $R = 1.5h$ to 0.89 at $R = 4h$. The difference grows rapidly for smaller R; at $R = h$, the ratio is 1.72. We will use both equations to derive $\langle V_R^2 \rangle^{1/2}$. Some care has to be exercised near radii where these terms approach zero and where, consequently, no asymmetrical drift is to be expected. For equation (10) this occurs at $R = 0.25h$ and at $R = 0.83h$ for the Q = constant case described in equation (13).

We emphasize that our analysis is based on an assumption of axial symmetry. This assumption enters both the determination of Q and the asymmetrical drift, because these rely on measurements of $V_{\rm rot}$, κ, A, and B. This is probably reasonable, because spiral structure is not expected to affect the systematic stellar motions by more than a few km s^{-1} and the ratio of velocity dispersions by more than 10%–20%. However, it must be a concern in similar work in ovally distorted or strongly barred systems, when it is even not at all obvious how to define $V_{\rm rot}$ or κ. Values for $V_{\rm rot}$ or Q determined in such galaxies (e.g., Kormendy 1984*a*, *b*) should be treated with caution.

III. OBSERVATIONS AND REDUCTIONS

The observations reported in this paper were obtained on 1983 June 13 and 14 with the 3.9 m Anglo-Australian Telescope, using the RGO spectrograph at the f/8 Cassegrain focus and the IPCS. The wavelength coverage was between 4786 and 5688 Å with channels spaced by 0.45 Å (25.9 km s^{-1}); the instrumental resolution is about 1.0 Å and corresponds to a velocity dispersion of about 20 km s^{-1}. The wavelength range covers as principal absorption lines the Mg *b* triplet and a number of Fe I lines, but also the emission lines Hβ and [O III]. The resolution along the slit was 2.″6 with a total usable extent of 2.′8. Flat field exposures were used to correct for pixel-to-pixel response changes, and twilight sky exposures were used to correct for vignetting effects along the slit in the spectrograph camera. Exposures of an argon arc were taken every 1500 s of exposure, and these were used to map the geometrical distortions of the observed arrays and to calibrate the wavelength scale. At each point between 4880 and 5610 Å, our rectified wavelength scale is accurate to an rms of 0.07 Å (4 km s^{-1}). Since we will use Hβ, we carefully mapped the distortion

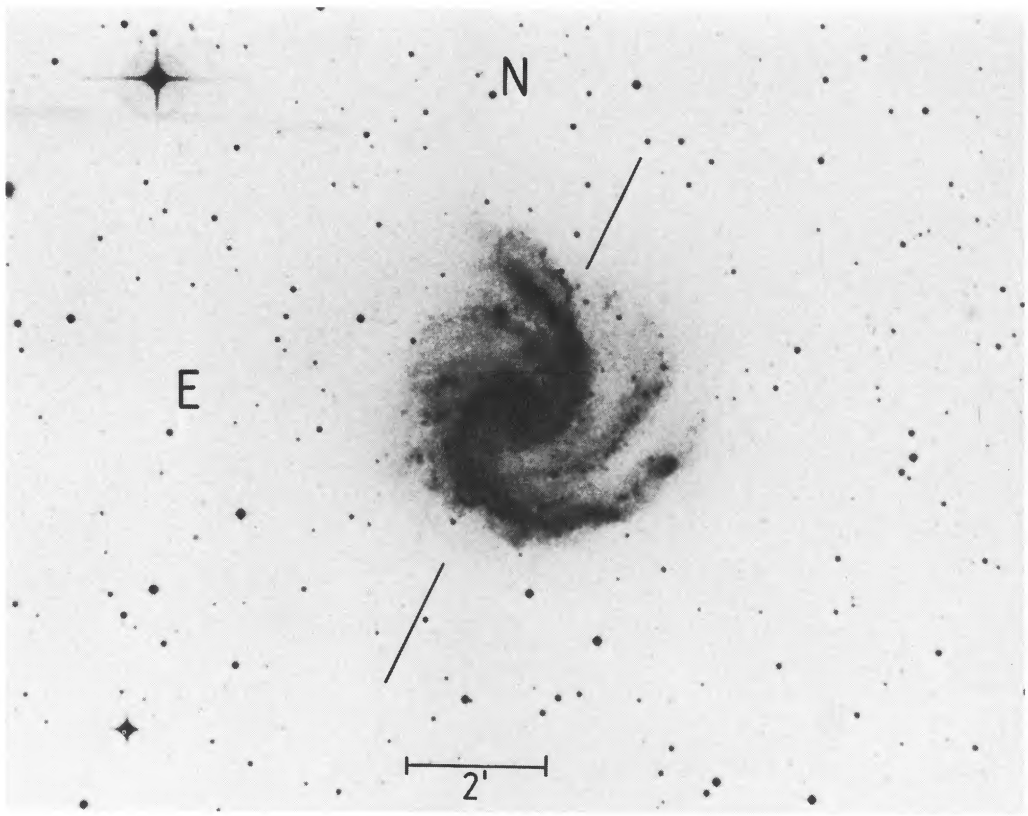

FIG. 1.—Reproduction of NGC 5247 from the SRC *J* survey. The orientation of the spectrograph slit during the observation is indicated. Galaxy data extend from 48″ southeast to 98″ northwest of the nucleus.

and wavelength scale for this part of the data arrays separately from strong nearby argon lines. This repeats well from measurement to measurement and is believed known to 0.05 Å (3 km s^{-1}), from its repeatability.

The systems observed are NGC 5247 and NGC 7184. NGC 5247 is an Sc(s)I–II galaxy (Sandage and Tammann 1981), which we have chosen because of its small bulge, regular spiral structures, and large areas of interarm region. A reproduction from the SRC *J* survey is given in Figure 1. Our spectrum was taken in position angle 155° (indicated in Fig. 1) and extended from 47″ southeast of the nucleus to 130″ northwest. The total exposure equalled 31,500 s (8.8 hr). The region beyond 107″ northeast of the nucleus was assumed to be sky background only; this is confirmed below from preliminary surface photometry. These nine spectra, which had an average of 125 counts per channel, were averaged and subtracted from the remaining spectra along the slit.

NGC 5247 is close to face-on. The width of the integrated H I profile at 20% of the peak is only 160 ± 10 km s^{-1} (Fisher and Tully 1981). Using its corrected radial velocity of 1216 km s^{-1} (Sandage and Tammann 1981) and a Hubble constant of 75 km s^{-1} Mpc^{-1}, we derive and adopt a distance of 16 Mpc. The integrated, corrected *B*-magnitude of 10.71 calculated by Sandage and Tammann then gives an absolute magnitude of -20.31 (2×10^{10} $L_\odot$) and Shostak's (1978) version of the Tully-Fisher relation predicts a width of the H I profile of 450 ± 50 km s^{-1}. The implied inclination is $20° \pm 3°$. If the velocity ellipsoid has the same shape as in the solar neighborhood, this inclination implies that our measured dispersion is about 5% higher than $\langle V_z^2 \rangle^{1/2}$ (see van der Kruit and Freeman 1984). We will not apply this correction.

Away from the nucleus we need to add small sections of the slit in order to attain a sufficient signal-to-noise ratio in the spectra. Of course we then need to correct for systematic velocity gradients along the slit. Since we did not know the kinematical major axis of NGC 5247, we chose our position angle to cover as much interarm as possible, and consequently we do find a measurable velocity gradient. We determine it from the emission lines which are seen over the full extent of the galaxy on the slit. It amounts to a mean slope of 1.2 km s^{-1} per pixel along the slit, and we applied the shifts necessary to correct for this.

The resulting set of spectra along the slit were added where necessary to increase the signal-to-noise ratio. The ranges in distance from the nucleus and average number of counts per channel are given in the first two columns of Table 1. The data within 20″ from the nucleus contain only 22,500 s of exposure, because during the remaining part of the exposure the seeing was very poor and would not allow the spatial resolution we are using near the nucleus. Fortunately, the galaxy is sufficiently bright at these positions.

We observed three template stars each during both observing nights. These are HD 118962 (K0 III), HD 119516 (G6 III) and HD 214987 (K0 III), and each exposure lasted between 1000 and 1500 s. Both spectral types are usable to fit old disk populations (see van der Kruit and Freeman 1984), and most of our reductions are based on the sum of the exposures of the K0 III stars HD 118962 and HD 214987. The radial velocities of the two stars are determined from their sharp Mg *b* and two Fe I lines as respectively $+3 \pm 3$ and $+9 \pm 3$ km s^{-1} heliocentric. The summed template spectrum of the four exposures has an average about 2000 counts per channel and is for all practical purposes free of noise.

The determination of radial velocity and velocity dispersion made use of the usual Fourier techniques. We used three different methods, all of which gave comparable results. In fact, our quoted uncertainties below are derived from the comparison of the results of these three methods and are our estimated 90% confidence errors. The first is to make use of the power spectra of the galaxy and template data (Illingworth and Freeman 1974). In this approach the radial velocity was determined first from the cross-correlation peak; this peak was found by determination where the derivative of the cross-correlation function changes sign. The second approach uses the cross-correlation method of Tonry and Davis (1979). The peak was fitted with a parabola, and the width was compared to that of the cross correlation of the two K0 III stars. The final approach was the Fourier quotient method of Sargent *et al.* (1977), which fits a

TABLE 1

SPECTRA ALONG POSITION ANGLE 155° IN NGC 5247

Distance from Nucleus	Mean Counts per Channel	V_{hel}[a] (km s^{-1})	$\langle V^2 \rangle^{1/2}$ (km s^{-1})	Peak in Hβ	V_{hel}[b] (km s^{-1})
Southeast 48″–35″	210	1359 ± 10	$\lesssim 25$	...	...
Southeast 35″–20″	410	1351 ± 10	37 ± 9	300	1348 ± 3
Southeast 20″–9″	670	1362 ± 7	52 ± 7	2010	1358 ± 2
Southeast 9″–4″	800	1359 ± 5	58 ± 7	3550	1357 ± 2
Southeast 4″–1″	930	1351 ± 5	52 ± 6	780[c]	1351 ± 5
Nucleus	1820	1346 ± 5	62 ± 6	330[c]	1350 ± 7
Northwest 4″–1″	1200	1343 ± 5	110 ± 10	530[c]	1348 ± 5
Northwest 9″–4″	710	1344 ± 6	46 ± 8	1490[c]	1340 ± 5
Northwest 20″–9″	460	1329 ± 7	42 ± 8	520	1335 ± 3
Northwest 35″–20″	330	1367 ± 10	68 ± 9	680	1338 ± 3
Northwest 61″–35″	550	1364 ± 6	31 ± 10	230	1322 ± 4
Northwest 79″–61″	600	1360 ± 5	32 ± 10	3320	1304 ± 2
Northwest 95″–79″	890	1367 ± 5	28 ± 11	8030	1296 ± 2
SE + NW 48″–35″	490	1361 ± 6	40 ± 9	...	...
SE + NW 35″–20″	740	1358 ± 5	56 ± 8	...	...

[a] After correcting for the velocity shift in the emission lines along the slit. The nucleus spectrum has not been shifted and only here do we have a "real" heliocentric velocity.

[b] Derived from the spectra before correction for the velocity gradient along the slit.

[c] The emission line sits in the middle of a broader Hβ absorption line. Velocity determination somewhat uncertain.

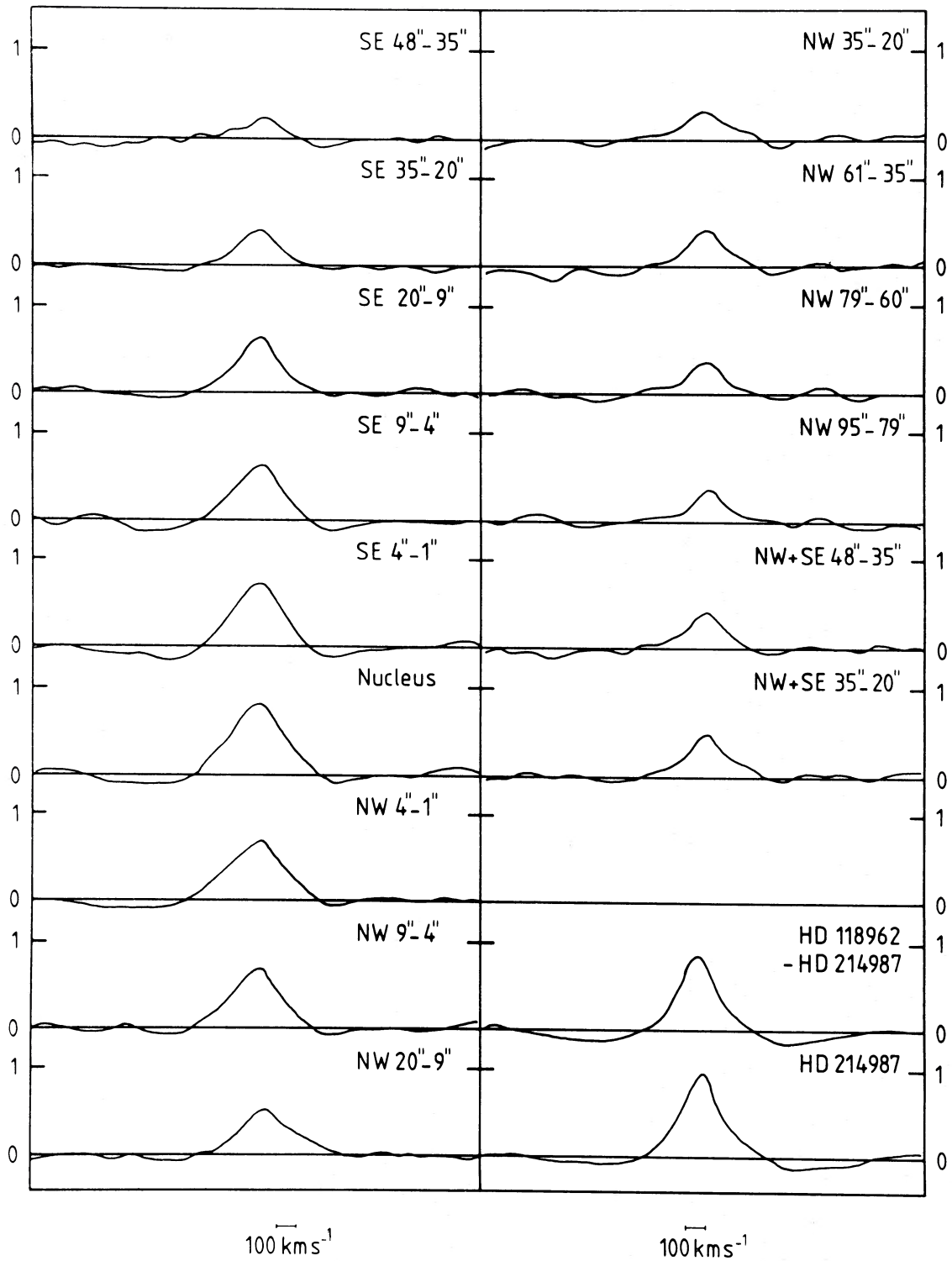

FIG. 2.—Cross-correlation spectra of the observations from NGC 5247 (p.a. 155°) with the sum of those of the two K0 III stars HD 118962 and HD 214987. The ranges of the slit over which data were added are indicated. We also show a cross correlation of the two individual K0 III stars and the autocorrelation function of our observation of HD 214987. The latter is artificially narrow due to correlated noise.

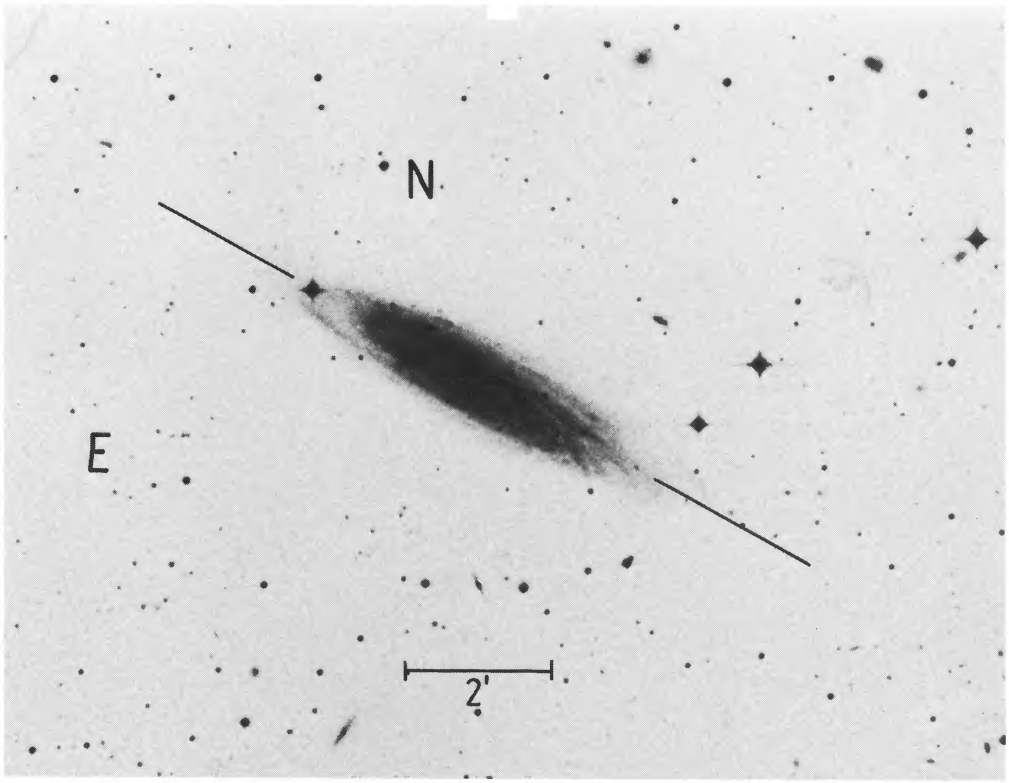

FIG. 3.—Reproduction of NGC 7184 from the SRC *J* survey. The orientation of the spectrograph slit during the observation is indicated. Galaxy data extend from 34″ southwest to 104″ northeast of the nucleus.

complex Gaussian to the quotient of the Fourier transforms of galaxy and template spectra. In all these methods the Fourier transforms were performed over the 1000 channels between 5041 and 5495 Å.

The quality of the data on NGC 5247 is illustrated in Figure 2, where we plot the peaks in the cross-correlation function of the galaxy spectra with that of the template sum. Because of the different geocentric velocities, the galaxy spectra were first shifted by -1320 km s^{-1} before the cross correlations were calculated. For comparison we also show the cross correlation of HD 118962 with HD 214987 and the autocorrelation function of the latter. The derived radial velocity and velocity dispersion are given in the third and fourth columns of Table 1, based on a straight average of the three methods mentioned above. In the final two columns we give the counts in the peak of the Hβ emission line relative to the nearby continuum and the derived radial velocity.

NGC 7184 is classified Sb(r)II by Sandage and Tammann (1981), and it is highly inclined and ranks as the tenth intrinsically brightest galaxy in the Revised Shapley-Ames Catalog. From the axis ratio on the SRC *J* prints we estimate an inclination of 75°. The corrected radial velocity of 2705 km s^{-1} (Sandage and Tammann 1981) leads us to adopt a distance of 36 Mpc. With this inclination it is unlikely that the vertical velocity dispersion has any significant influence on our measurement.

We observed NGC 7184 mainly in position angle 60°, which is very close to the major axis (see Fig. 3). The measurements extended from 144″ northeast of the nucleus to 34″ southwest, and the total exposure equalled 25,500 s (7.1 hr). The region beyond 114″ northeast of the nucleus was assumed to be sky background only; this is also confirmed by the preliminary surface photometry (see below). These 10 spectra, which had an average of 117 counts per channel, were averaged and subtracted from the remaining spectra along the slit.

We also took an exposure in position angle 180° centered on the nucleus; the total exposure time is 3000 s (0.8 hr). In this spectrum the regions beyond 47″ on either side of the nucleus were used as sky background exposures. These 32 spectra have an average of 14 counts per channel.

The resulting spectra were analyzed in the same way as described for NGC 5247 above; the results are given in Table 2. Figure 4 illustrates the peaks in the cross-correlation functions; this time the galaxy spectra were shifted first by -2588 km s^{-1} to allow for the different geocentric velocities of galaxy and template.

In analyzing our observational results we make the assumption that what we are measuring is the old disk population. In loose terms, we mean by this for the solar neighborhood those stars in the disk older than, say, a few Gyr. According to Jahreiss and Wielen (1983), such stars have velocity dispersions $\langle V_R^2\rangle^{1/2} \approx 40$ km s^{-1}, $\langle (V_\theta - V_t)^2\rangle^{1/2} \approx 30$ km s^{-1}, and $\langle V_z^2\rangle^{1/2} \approx 25$ km s^{-1}, with only a small dependence on the age of the various constituent generations. The light of such a population is dominated by its red giants (and to a lesser extent subgiants), in agreement with our actual spectra.

We also need to consider contributions of other populations to our spectra. Young stars are generally of little concern: they are either dwarfs and do not contribute significantly to the surface brightness, or are hot, young stars in the spiral arms, and these do not display the spectral lines in our template spectra. A component to consider is that of a "thick disk," as proposed by Gilmore and Reid (1983) in our Galaxy. Such a component would be of older age and therefore contain red giants, and it would display a rather high velocity dispersion. In our Galaxy, and presumably also in other systems with not very prominent bulges (such as NGC 5247 and 7184), the face-on surface brightness is low, namely, only 10% of that of the old disk population. Also taking into account that it *may* have a lower metallicity than the old disk, we conclude that the effects on our spectra are very likely to be negligible.

Our interpretation of these data require photometric parameters of these systems; however, surface photometry of neither of them is available in the literature. We have therefore

TABLE 2

SPECTRA ALONG POSITION ANGLES 60° AND 180° IN NGC 7184

Distance from Nucleus	Mean Counts per Channel	V_{hel} (km s^{-1})	$\langle V^2\rangle^{1/2}$ (km s^{-1})	Peak in Hβ	V_{hel} (km s^{-1})
p.a. 60°					
Northeast 104″–81″	220	2803±15	...	560	2838±5
Northeast 81″–57″	440	2815±10	56±30	490	2851±5
Northeast 57″–47″	370	2797±12	124±30	430	2825±5
Northeast 47″–36″	360	2801±10	135±30	170	2838±9
Northeast 36″–21″	500	2802±10	169±20	...	...
Northeast 21″–10″	820	2707±6	170±15	...	...
Northeast 10″–5″	980	2667±5	240±15	...	...
Northeast 5″–2″	950	2641±5	229±20	...	...
Northeast 2″–0″	1850	2612±5	158±15	...	...
Southwest 2″–0″	1680	2529±5	132±15	...	...
Southwest 5″–0″	900	2462±6	115±20	...	...
Southwest 10″–5″	830	2469±7	113±20	...	...
Southwest 21″–10″	820	2438±7	125±15	...	...
Southwest 34″–20″	460	2379±10	71±20	...	...
p.a. 180°					
South 26″–12″	80	...	...	40	2551±5
Nucleus	490	2581±7	135±20	...	...
North 26″–12″	60	...	...	30	2603±5
North 40″–26″	40	...	...	30	2616±5

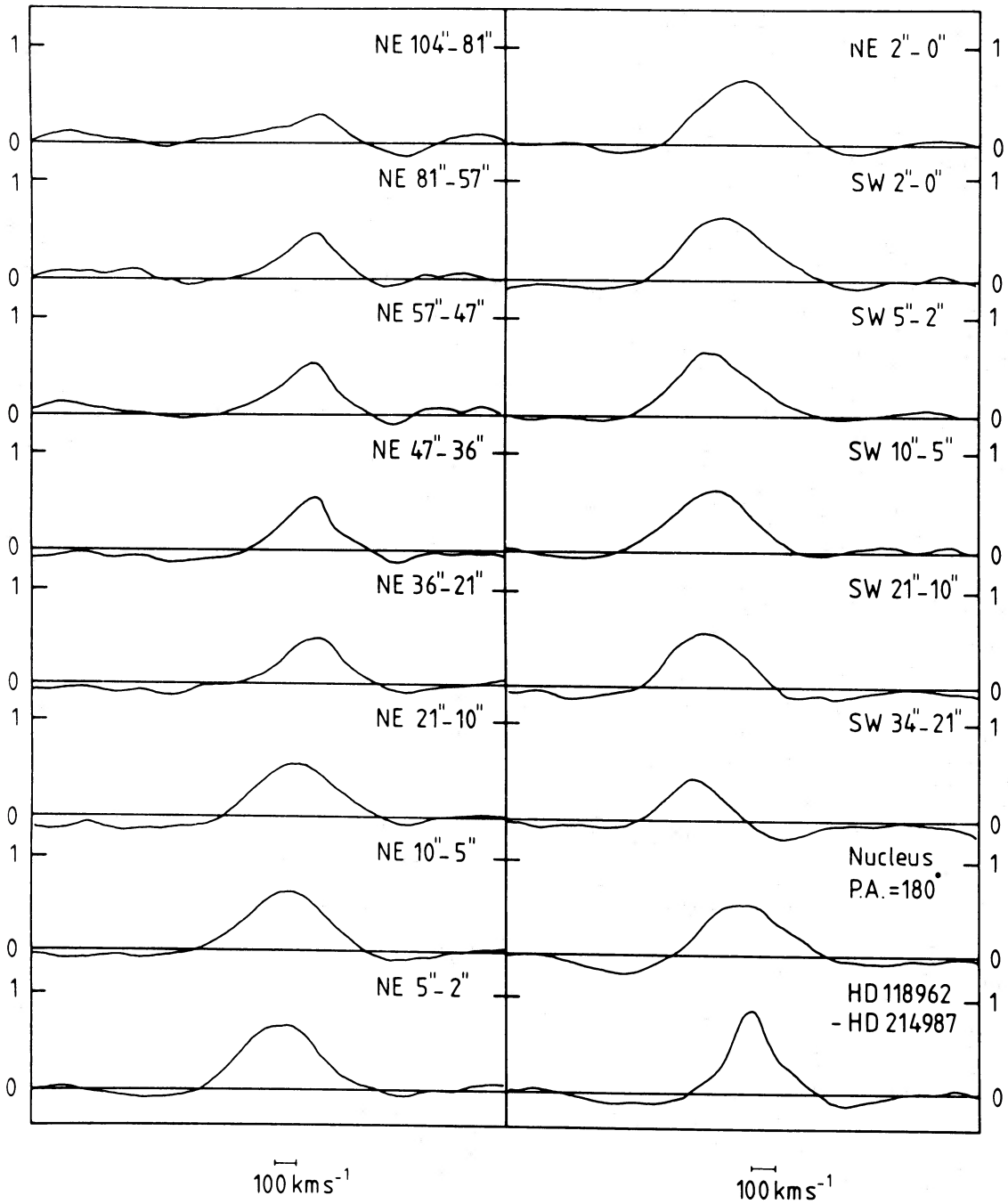

FIG. 4.—Cross-correlation spectra of the observations of NGC 7184 (p.a. 60°) with the sum of those of two K0 III stars. These stars and the presentation are the same as in Fig. 2.

derived preliminary surface photometry from the film copies of the SRC *J* southern sky survey. NGC 5247 can be found on plate 577 (from which we also scanned NGC 5170, the subject of a further paper on the subject), and NGC 7184 on plate 601. The plates were digitised with the ASTROSCAN of Leiden Observatory and reduced as described in, e.g., van der Kruit (1979) and van der Kruit and Searle (1981*b*). The characteristic curves were derived using the intensity ratios of the calibrator steps as given in the UKSTU handbook. In the linear part, the characteristic curves have slopes γ of about 3.5 (density–log exposure).

The magnitude scales were calibrated by simulation of the aperture photometry given for the galaxies by Longo and de Vaucouleurs (1983). Because of the deep exposures, annular apertures had to be formed. Using three of these on NGC 5170 and three on NGC 5247, we find a sky brightness for plate 577 of $\mu_B = 22.54 \pm 0.21$ mag arcsec^{-2}. From five annular apertures on NGC 7184, the sky brightness of plate 601 was found to be $\mu_B = 22.39 \pm 0.16$ mag arcsec^{-2}. From the consistency of this value from various apertures and the reasonable values derived, we conclude that this preliminary surface photometry is adequate for our purposes.

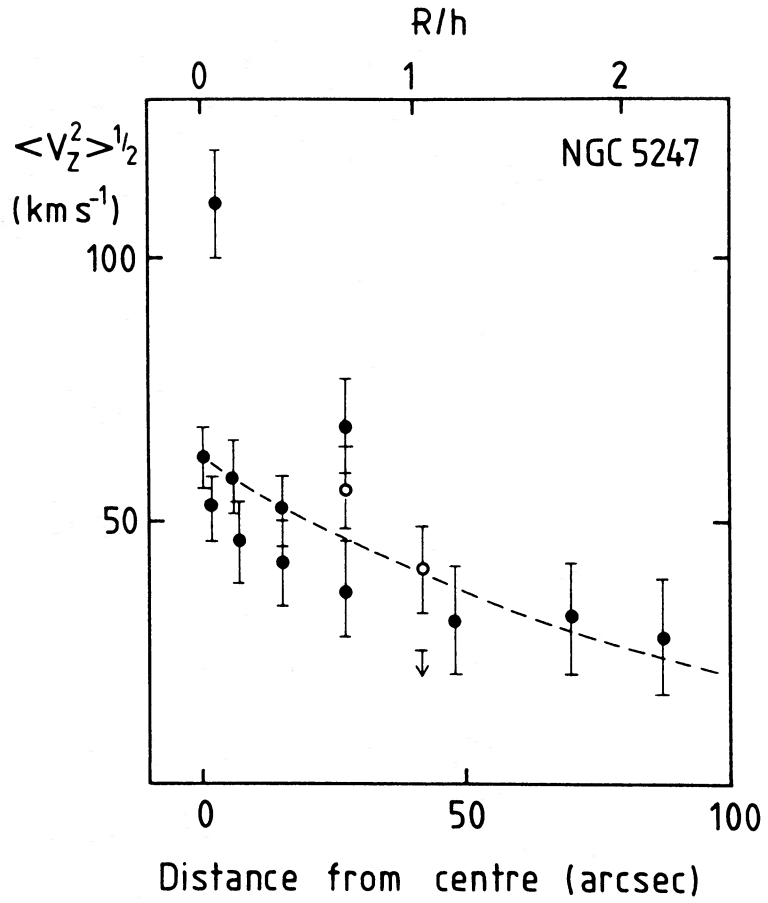

FIG. 5.—Measurements of the vertical velocity dispersion $\langle V_z^2 \rangle^{1/2}$ of the old disk population in NGC 5247. The dashed line is the fit given by eq. (14). The open circles are the solutions after adding the data at the same distance ranges on either side of the nucleus.

We analyze the surface brightness maps in terms of a simple exponential disk. The azimuthally averaged profile of NGC 5247 gives a scale length of 40″ (3.1 kpc), and by combining interarm areas from radial profiles in various position angles, we estimate a similar scale length for the old disk population. The central extrapolated surface brightness in B (corrected to face-on) is 20.9 mag arcsec^{-2} for the whole disk and 21.9 mag arcsec^{-2} for the old disk only. These surface brightnesses have uncertainties of a few tenths of a magnitude. From the annular apertures we find that the disk of NGC 5247 has $U-B \approx 0.05$ and $B-V \approx 0.55$. The region where we determined the sky spectrum is fainter than 22 mag arcsec^{-2}; the region where we measured is at least 2 mag brighter, and no large systematic errors are to be expected from our procedure. The radial light profile does not require the presence of a bulge component in the central part. In our analysis of NGC 5247 we will treat it as a pure-disk system.

For NGC 7184 we only use the profile for the total disk beyond the ring at ~45″ from the center. The scale length is about 48″ and the central extrapolated, face-on surface brightness $\mu_B = 22.2$ mag arcsec^{-2}. Beyond about 180″ (3.8h) the surface density drops very steeply, reminiscent of the sharp edges in edge-on systems (van der Kruit and Searle 1981a). The annular apertures give a disk color for NGC 7184 of $U-B \approx 0.10$ and $B-V \approx 0.70$. The star 160″ northeast of the nucleus of NGC 7184 was actually recorded on our slit, but beyond the area where the lines from the arc lamp could be exposed. It is from this that we derive our pixel separation on the sky of 2.″6.

NGC 5247 and 7184 have Galactic latitudes of respectively 44° and 51°, and Galactic extinction is therefore expected to be small, certainly compared to the uncertainties in the surface brightness. We will neglect its effects. As indicated above, our assumed distances to the two galaxies are based on a Hubble constant of 75 km s^{-1} Mpc^{-1}.

IV. $\langle V_z^2 \rangle^{1/2}$ AND THE MASS DISTRIBUTION

We first address the question of the vertical velocity dispersion and the mass distribution in the disk. As explained in § II, we expect on the basis of the constant thickness model of van der Kruit and Searle (1981a) and a constant mass-to-light ratio with radius that the vertical velocity dispersion drops off with distance from the center as an exponential with twice the scale length of the light distribution (see eq. [3] above). We can then use equation (2) to convert to surface densities, if z_0 is assumed.

In Figure 5 we have plotted the points from Table 1 on NGC 5247. The open circles are from the solutions at the bottom of the table, where similar distance ranges on either side of the nucleus have been added together. The most obvious deviating point is the one at 1″–4″ northwest, which is much higher than all the others. The relative broadness of the lines in this spectrum compared to the neighboring ones is even obvious in a visual inspection. The cross-correlation spectrum is also well

defined. There is no reason to suspect this measurement, and we cannot offer an explanation for its behavior.

We made a least-squares solution of all the points in Figure 5 to an exponential with radius. The result, which is illustrated with the dashed line, is

$$\langle V_z^2 \rangle^{1/2} = (62 \pm 7) \exp [-(0.42 \pm 0.10) R/h] \text{ km s}^{-1} . \quad (14)$$

The value of the exponential slope of 0.42 ± 0.10 is in excellent agreement with the predicted 0.50 of equation (3). However, the "error" of 0.10 is only the formal standard error of the fit and does not properly take the error bars in Figure 5 into account. Furthermore, deleting the discrepant point at 1″–4″ northwest gives 0.35 ± 0.09. Taking this into account still leaves the fact that for R/h between 0 and 2 the velocity dispersion has dropped from ~ 60 to ~ 30 km s^{-1}, and considering the error bars, this is consistent with a drop by a factor of e. We conclude that our results give clear evidence that the vertical velocity dispersion is falling with radius and that the e-folding is consistent with but does not strongly demand a constant M/L. For the exponential slope of 0.42 given in equation (14), M/L increases by a factor of 1.4 over the range of R/h observed.

Requiring the velocity dispersion to drop off with a scale length of $2h = 80''$ gives an extrapolated value for the central dispersion of 67 ± 20 (rms) km s^{-1} (or 64 ± 15 km s^{-1} if the point at 1″–4″ northwest is deleted). In order to calculate a surface density, we need to assume a value for z_0, while we will also assume it to be constant with radius. Note that this is observed to be the case even near the center in bulgeless edge-on spirals (van der Kruit and Searle 1981*a*, 1982). As in van der Kruit and Freeman (1984), we will take 0.7 ± 0.2 kpc, following the result of van der Kruit and Searle (1982); the resulting ratio of 4.4 for h/z_0 is also well inside the range found for seven edge-on systems in the latter reference. It is then easy to find the surface density distribution in NGC 5247 as (300–750) exp $(-R/3.1$ kpc) $M_\odot$ pc^{-2} and a total mass for the disk of 2–5 $\times 10^{10}$ $M_\odot$. The extrapolated central surface brightness of 21.7 mag arcsec^{-2} for the old disk population corresponds to 110 $L_\odot$ pc^{-2}. The resulting M/L for the old disk population is (3–7) $M_\odot/L_{\odot,B}$. This is consistent with the range (5–10) found in van der Kruit and Freeman (1984). Including the young population, the M/L for the whole disk becomes (1–2.5) $M_\odot/L_{\odot,B}$.

It has been emphasized previously (van der Kruit 1983; van der Kruit and Freeman 1984; van der Kruit and Shostak 1984) that these M/L ratios and disk masses are too low to explain the amplitude of the observed rotation curves. The conclusion is that the disks contain only about one-third of the mass out to the optical edge as indicated by the rotation curve. This conclusion has recently been extended to more moderately inclined systems by Wevers (1984) as a result of the Palomar-Westerbork Survey of bright spiral galaxies. His sample consists of spirals of various Hubble stages for which he obtained surface photometry in three colors and H I synthesis observations. Wevers takes the mean value of 7 for the M/L of the old disk population and simply scales this with the observed color index of the disk to find its "total" M/L, using population models as in Searle, Sargent, and Bagnuolo (1973) or Larson and Tinsley (1978). For his set of 16 systems, he then finds that the disks contain $29\% \pm 16\%$ of the mass out to the optical radius.

Recently, Efstathiou, Lake, and Negroponte (1982) have studied numerically the stability of particular models that probably represent actual galaxies reasonably well. Their models contain an exponential disk embedded in a halo such that the rotation curve of the model galaxy is flat. They parameterize their models by a parameter which—following Sellwood (1983)—we will call Y and which equals $V_{\rm rot}(h/GM_D)^{1/2}$, where M_D is the mass of the disk and $V_{\rm rot}$ the rotation velocity in the flat part. They find that their models are stable against global, barlike disturbances if the condition

$$Y = V_{\rm rot}(h/GM_D)^{1/2} \gtrsim 1.1 \quad (15)$$

is fulfilled.

Values for M_D, h, and $V_{\rm rot}$ have been listed for eight edge-on galaxies (including our own) by van der Kruit and Searle (1982) based on $(M/L)_{\rm old\ disk} = 7$. For these systems, the value of $Y = 0.90 \pm 0.09$ (rms). This suggests that $(M/L)_{\rm old\ disk} \approx 5$ is required, unless all these edge-ones are actually strongly barred.

We may also use Wevers' sample, which is also based on $(M/L)_{\rm old\ disk} = 7$. His data give for the parameter Y a value of 0.98 ± 0.27. This sample is made up almost entirely of non-barred systems. Both samples suggest that the value for $(M/L)_{\rm old\ disk}$ of 7 is too high in order to conform to the criterion. However, using the lower limit of our range of (5–10) $M_\odot/L_{\odot,B}$ for the old disk population would raise the mean value of the stability parameter to the required value of ~ 1.1.

If we estimate the surface density in the solar neighborhood as (80 ± 20) $M_\odot$ pc^{-2} (see above), the surface brightness of 15 $L_{\odot,B}$ pc^{-2} gives an $(M/L)_{\rm old\ disk}$ for our Galaxy of (6 ± 2) $M_\odot/L_{\odot,B}$. Including our value of (5 ± 2) $M_\odot/L_{\odot,B}$ for NGC 5247 together with the 8 ± 4 (NGC 891), 8 ± 5 (NGC 628), and 4 ± 3 (NGC 1566) in van der Kruit and Freeman (1984), a range 6 ± 2 $M_\odot/L_{\odot,B}$ is suggested as the best estimate. The 5 $M_\odot/L_{\odot,B}$ required by Efstathiou *et al.*'s stability criterion then is consistent, within the uncertainties, with our observational results. Although a Hubble constant of 50 km s^{-1} Mpc^{-1} would reduce our inferred M/L by 30%, the actual values of Y remain unaffected by a different distance scale.

To conclude this section we note that the "best" estimates for Y are the ones we can calculate for our Galaxy and NGC 891. This is so because in these systems we have actually determined the disk mass from the dynamics without having to assume a value for $(M/L)_{\rm old\ disk}$, while $V_{\rm rot}$ does not depend on an inclination correction. For the Galaxy we use the local surface density of (80 ± 20) $M_\odot$ pc^{-2} and a scale length of 4.5 ± 0.5 kpc; the disk mass then is $6 \pm 2 \times 10^{10}$ $M_\odot$. With $V_{\rm rot} = 235 \pm 15$ km s^{-1}, this gives $Y = 0.98 \pm 0.25$. In NGC 891 we use the parameters summarized in van der Kruit (1983), namely $h = 4.9$ kpc and $M_D = 5 \pm 1 \times 10^{10}$ $M_\odot$. With $V_{\rm rot} = 225 \pm 10$ km s^{-1}, we then have $Y = 1.07 \pm 0.12$. Both galaxies seem to be only just stable to global barlike modes, although the observational errors do not rule out at all that the condition is actually *not* fulfilled.

V. $\langle V_R^2 \rangle^{1/2}$ AND THE LOCAL STABILITY

The observational results on NGC 7184 in Table 2 have been plotted in Figure 6. The Hβ point at the nucleus comes from the spectrum in position angle 180°. Note that this point is nicely consistent with those in position angle 60°; no difference in the stellar velocity scales appears to exist. We can also look at the Hβ velocity scale; the values observed in position angle 180° suggest a systematic velocity of about 2577–2580 km s^{-1}, in excellent agreement with the stellar velocity scale. In the following we use a systemic velocity of 2581 km s^{-1}.

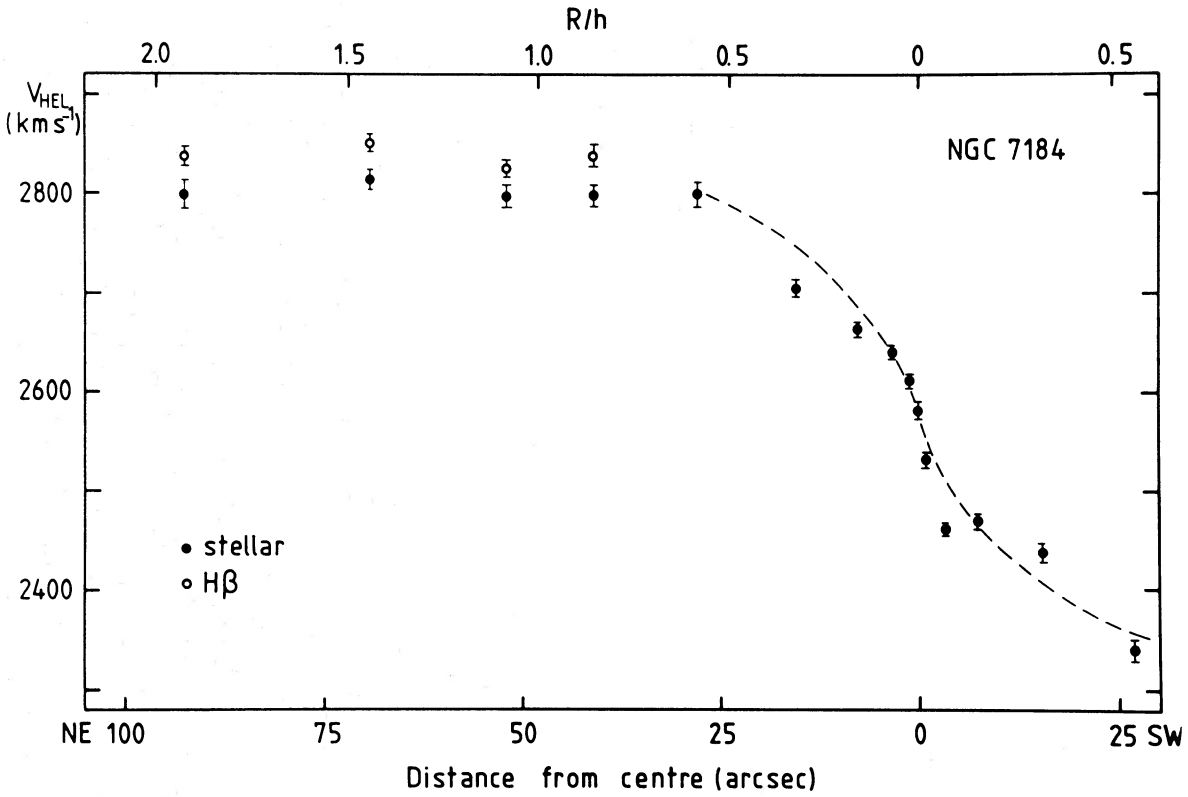

FIG. 6.—The gaseous and stellar rotation curve of NGC 7184. The data have not been corrected for inclination or for line-of-sight effects. The flat rotation curve and the asymmetrical drift are evident. The dashed line shows a symmetric stellar rotation curve for the central areas.

Both the stellar and gaseous velocities in position angle 60° show a rotation curve which is essentially flat beyond $R/h \approx 0.5$ (25″). From the Hβ points we derive a mean rotation velocity at these radii of 266 ± 10 km s^{-1}, after correction for an inclination of 75°. The uncertainty in V_{rot} is roughly equal to possible departures from circular motion as due, e.g., to spiral density waves. The magnitude of the effect on the derived parameters then is included in the quoted errors. In what follows we will use this value over the range where Hβ has been observed, and we will take $A = -B = V_{rot}/2R$. This also implies that we should use equations (10) and (13) for our analysis of the asymmetrical drift. The data in Figure 6 show that an asymmetrical drift has actually been observed between $0.8h$ and $2.0h$.

Next we inquire into the effects of line-of-sight integration on the stellar velocities and velocity dispersions. These can be estimated from numerical tests, where we will always assume cylindrical rotation (i.e., V_{rot} and the velocity dispersion in the old disk population are not functions of z). The major axis is a somewhat special position, in that the parts of the line of sight in front of and beyond the disk's symmetry plan have identical contributions. This will in any case mean that our methods of data reduction are likely to underestimate the stellar velocities and tend to enhance the observed magnitude of the asymmetrical drift. On the other hand, absorption in a thin central dust layer will not be of much concern in this situation.

We started using preliminary values for V_t and the velocity dispersion and assumed a ratio h/z_0 of 4. The resulting observed profiles were then calculated and compared to the actual ones at the corresponding positions. The corrections in V_t were small, but not negligible, as expected. They ranged from around 3 km s^{-1} at $2.5h$ to 9 km s^{-1} at $0.9h$. The profiles were still closely Gaussian, and the velocity dispersions were 5%–10% higher than the assumed $\langle (V_\theta - V_t)^2 \rangle^{1/2}$ at the observed positions. All these corrections were applied. In all this we always used $i = 75°$ and $\langle (V_\theta - V_t)^2 \rangle^{1/2} / \langle V_R^2 \rangle^{1/2} = 0.71$, as required by the flat rotation curve. From a numerical simulation of our observations, we also checked that it is correct to let our values apply to the middle of the ranges in R over which spectra were added.

It is now possible to calculate values for $\langle V_R^2 \rangle^{1/2}$ and Q. In order to estimate an uncertainty in the dispersion, we will use $h = 48'' \pm 5''$. As indicated above (§ III), the color index in the disk is $(B-V) \approx 0.70$, $(U-B) \approx 0.10$. These are rather red colors, and on the basis of population models we may assume that M/L is not very different from that of an old disk population. The absence of large numbers of young stars in the disk of NGC 7184 is also indicated by the fact that it took as long an exposure as ours to even record the Hβ emission line. Consequently, we will use $M/L = 5$ and on this basis estimate a central surface density of $450 \pm 50\ M_\odot\ \mathrm{pc}^{-2}$.

We then arrive at values for $\langle V_R^2 \rangle^{1/2}$ and Q as given in Table 3 for the case that the ratio $\langle V_R^2 \rangle^{1/2} / \langle V_z^2 \rangle^{1/2}$ is constant (Case A and eq. [10]) and the case that Q is constant (Case B and eq. [13]). The error in Q is larger than that in $\langle V_R^2 \rangle^{1/2}$ due to the large uncertainty in assumed M/L and therefore surface density. The quoted uncertainties are roughly 90% confidence levels. In the latter case we run into a difficulty at our smallest value for R/h, because it is close to the radius where the term between parentheses in equation (13) equals zero. We would not expect a measurable asymmetrical drift here for the Q = constant situation. On the other hand, at about this

TABLE 3

VELOCITY DISPERSIONS AND TOOMRE Q's IN NGC 7184[a]

	R			
PARAMETER	104″–81″	81″–57″	57″–47″	47″–36″
R (kpc)	18.2–14.1	14.1–10.0	10.0–8.2	8.2–6.3
R/h	2.2–1.7	1.7–1.2	1.2–1.0	1.0–0.75
V_t	233±15	247±10	230±12	238±10
Case A (eq. [10]):				
$\langle V_R^2\rangle^{1/2}$	71±10	65±15	102±15	108±20
Q	1.7±0.5	1.5±0.5	1.9±0.5	2.1±0.6
Case B (eq. [13]):				
$\langle V_R^2\rangle^{1/2}$	72±15	76±20	150±55	...
Q	1.7±0.5	1.6±0.5	2.9±1.3	...
Profile width:				
$\langle V_R^2\rangle^{1/2}$	...	80±40	160±40	165±40
Q	...	1.6±0.8	3.2±1.8	3.1±1.3
Assume $\langle V_R^2\rangle^{1/2} = 180\ exp(-R/2h)$ *km s*$^{-1}$:				
$\langle V_R^2\rangle^{1/2}$	70	90	104	118
V_t	233	228	228	232
Q	1.7	1.8	2.0	2.2
Assume $Q = 2.0$ *at all radii*:				
$\langle V_R^2\rangle^{1/2}$	83	102	105	105
V_t	221	230	249	264

[a] All values of V in km s^{-1}. In these calculations we have always assumed that $V_{rot} = 266\pm10$, $A = -B$, $M/L = 5\ M_\odot/L_{\odot,B}$, $\sigma(0) = 450\pm50\ M_\odot\ pc^{-2}$, and $h = 48''\pm5''$.

radius the luminosity profile starts to deviate from the exponential that applies at larger radii, so that this prediction should not be taken too seriously. Also, at small radii departures from a strictly flat rotation curve have a larger effect.

We first check on consistency with our assumptions. The solution for case A can be fitted indeed within the errors with $\langle V_R^2\rangle^{1/2} \propto \exp(-R/2h)$ if the extrapolated velocity dispersion at $R = 0$ is about 180 km s^{-1}. It should be emphasized that we do not really predict the radial dependence to apply all the way to the nucleus and that this value is not an expected one when a measurement could be made at the position of the nucleus. This is because NGC 7814 has a bulge which must alter the dynamics. Case B is only marginally verified by our derived values for Q. The data at the three largest values of R are all consistent with $Q \approx 2.2$, but the fact remains that we expect to measure a small asymmetrical drift at the innermost position, where our V_t of 238±10 km s^{-1} is strictly inconsistent with the V_{rot} of 266±10 km s^{-1}. However, we consider this as yet not to be compelling evidence against the Q = constant case.

The next two lines in Table 3 give for three distances the velocity dispersions and Q's on the basis of the observed profile widths. The latter were corrected for the line-of-sight effects as determined above to give the tangential velocity dispersion and were then multiplied by $2^{1/2}$ to give $\langle V_R^2\rangle^{1/2}$ based on the expected ratio from the observed flat rotation curve. It is seen that these agree with both cases above from the asymmetrical drift equation, although only marginally so for case A at small R.

We finally illustrate strict solutions according to the assumptions guided by the experience just described. The first is for the case that $\langle V_R^2\rangle^{1/2} = 180\ \exp(-R/2h)$ km s^{-1}, which seems the best compromise to fit both our values of V_t and the profile width. In that solution, Q increases from 1.7 at about two scale lengths to 2.2 just within one scale length. The second one is for the case that $Q = 2.0$ at all radii, which is also consistent with the data except for the asymmetrical drift at the smallest R.

It may be useful for comparative purposes to find the best value for Q in the solar neighborhood. We will use the value of $80\pm20\ M_\odot\ pc^{-2}$ (see above) for the local surface density. For the rotation velocity a value of 235±15 km s^{-1} brackets the values currently used throughout the literature, while the same is true for a distance to the centre of 8.5±1.0 kpc. For a flat rotation curve this corresponds to $A = -B = (13.8\pm1.9)$ km s^{-1} kpc^{-1} and $\kappa = 39\pm5$ km s^{-1} kpc^{-1}. Again from Jahreiss and Wielen (1983) we find for the local old disk population $\langle V_R^2\rangle^{1/2} = 45\pm5$ km s^{-1} and $\langle (V_t - V_\theta)^2\rangle^{1/2} = 30\pm5$ km s^{-1}. Their ratio should be 1.41 for a flat rotation curve, so we see that the two values are indeed consistent with this. The values adopted then result in $Q = 1.5\pm0.5$.

Our results for NGC 7184 show Q to be in the range 1.7–2.2 over the range $R/h = 0.8$–2.0. Although we find it difficult to fit our data for Q = constant, it nevertheless remains true that our "case A" solution does not give a *large* variation in Q. The indicated behavior is certainly also consistent with recent findings in numerical experiments. Efstathiou, Lake, and Negroponte (1982) find that their models heat up to final values of $Q \approx 1.5$–2 for $R/h \lesssim 3$. Similarly, Sellwood and Carlberg (1984) find that their simulations result in equilibrium values for $Q \approx 2$ at all radii.

We have shown in § IV that the halo masses seem to be sufficiently large to provide global stability to the disks. The result for NGC 7184, however, indicates that the velocity dispersion of the stars in the central regions is certainly fairly substantial. In effect, at $R \approx 1h$ it is roughly 40% of the local rotation velocity. Now, this value may be influenced by the actual deviations locally from the assumed exponential behavior of the disk; but it nevertheless will be true that the velocity dispersion is not very small compared to the local value of V_t. This is relevant because Sellwood (1983) has concluded that a large amount of random motion near the center is very effective in reducing the growth rate of instabilities. We therefore propose that our derived large values of $\langle V_R^2\rangle^{1/2}$ in the inner regions of NGC 7184 suggest that random motions of the stars in the disks are also important in providing global stability to the disks. So, even if—as indicated at the end of § IV—the halo masses are *not* sufficient to stabilize the disks (as the observational errors after all allow), we still can resort to the velocity dispersions in the old disk population in the inner regions.

Finally, we compare our results to recent work by Kormendy (1984*a*, *b*). In the S0 galaxy NGC 1553, which has a pronounced lens, he finds $Q \approx 3$. The bar of NGC 936 (SB0) has $Q \approx 3$, and the disk $Q \approx 7$. Kormendy notes that this is consistent with the idea that S0 disks are too hot to have small-scale structure. In the Sb system NGC 488, Illingworth and Kormendy (quoted in Kormendy 1984*b*) find Q in the range 2–4.4, which is taken by these authors as the reason why this system shows no large-scale ("grand design") spiral structure. However, they used M/L values based on the Larson and Tinsley (1978) models, which give $M/L_B \approx 4$ for $B-V = 0.8$. Our results on the old disk population show that these might be somewhat too low (an old disk population has about the color index just mentioned, and we find a corresponding $[M/L]_{\text{old disk}}$ of 6±2). Taking this into account, we suggest that their measurement would also give $Q \approx 2$ for NGC 488 as the

best solution when our M/L is used. Similarly, the large values of Q in the disk, lens, and bar of NGC 1553 and NGC 936 will also come out 30% lower if $M/L = 6$ based on an old disk population is used rather than $M/L = 4$ for a Larson and Tinsley model of the same color index.

VI. DISCUSSION AND CONCLUSIONS

From the analysis above, it appears that spiral galaxies in general have sufficient halo mass and sufficient velocity dispersion in their disk stars to avoid most of the global and local instabilities. We first comment in this section on implications for galactic structure and then summarize our results.

In the first place, we comment on unseen matter in the disks. From Bahcall's (1984*b*) study of the solar neighborhood, it follows that the Galactic disk there has a surface density of *observed* material of about 50 $M_\odot$ pc^{-2}. This is lower than his and our dynamical surface density of 80 ± 20 $M_\odot$ pc^{-2} in case any unobserved disk material has the same velocity dispersion as the old disk population. The situation described by, e.g., Oort (1965) still persists, that a substantial fraction of the disk mass is unobserved. Bahcall finds that this is even about 50% in terms of the local *space* density at $z = 0$. Since our $(M/L)_{\text{old disk}}$ in the solar neighborhood is comparable to external systems, we are forced to conclude that this situation applies also in other galaxies.

We may also phrase this as follows. The old disk in, e.g., NGC 891 has a $B-V \approx 0.8$, $U-B \approx 0.2$. Using an initial mass function estimated for the solar neighborhood with a lower mass limit of 0.1 $M_\odot$, Larson and Tinsley (1978) give an M/L_B corresponding to these colors about 2.5–3.5 $M_\odot/L_{\odot,B}$. Our observed $(M/L)_{\text{old disk}}$ in NGC 891 of 8 ± 4 $M_\odot/L_{\odot,B}$ then also implies that the luminosity function of the local disk population is incapable of explaining our observed M/L. This luminosity function must be greatly in error or not generally applicable, if we are to avoid the conclusion that the old disks contain large amounts of matter in a form other than hydrogen-burning main-sequence stars. Our work extends the presence of locally "missing" mass to disks of other spiral galaxies.

We also ask the question as to what fraction of the total mass generally resides in the disk. We will use the total mass of the galaxy out to the edge of the disk $R_{\max}$. Of course, this fraction is reflected in the value of the parameter Y of Efstathiou, Lake, and Negroponte (1982). The relation of Y to the halo-to-disk mass as a function of radius has been illustrated rigorously by Sellwood (1983, Fig. 1*a*). Here we derive an approximate relation, where all masses are those inside the disk edge $R_{\max}$. In an excellent approximation, the disks have a total mass for $R_{\max}/h \gtrsim 4$–5 of

$$M_D = 2\pi h^2 \sigma_0 , \tag{16}$$

and essentially all this mass resides inside $R_{\max}$. When there is no mass outside the disk, this would result in a rotation curve with maximum rotation velocity

$$V_{\text{disk}} = 0.83(\pi G h \sigma_0)^{1/2} \tag{17}$$

(see van der Kruit and Searle 1982, Appendix) for $h/z_0 \approx 4$. Here σ_0 is again the central surface density. Such a disk has an essentially flat rotation curve from $R \approx 1.5h$ out to the truncation radius (van der Kruit and Searle 1982, Fig. A1). A halo then would also by itself produce a roughly flat rotation curve with amplitude $V_{\text{halo}} = (V_{\text{rot}}^2 - V_{\text{disk}}^2)^{1/2}$ and have a mass interior to $R_{\max}$ of

$$M_M(R_{\max}) \approx \frac{e}{\sin^{-1} e} \frac{R_{\max}}{h} \frac{V_{\text{halo}}^2 h}{G} , \tag{18}$$

where $(1 - e^2)^{1/2}$ is the halo axis ratio. Then we can write

$$\frac{M_H(R_{\max})}{M_D} \approx \frac{e}{\sin^{-1} e} \frac{R_{\max}}{h} [Y^2 - 0.344] . \tag{19}$$

We may use a roughly spherical halo, so that $e/\sin^{-1} e \approx 1$, and we will take $R_{\max}/h \approx 4$ (van der Kruit and Searle 1982). The condition $Y \gtrsim 1.1$ then translates into $M_H(R_{\max})/M_D \gtrsim 3.5$. For our two samples in § IV, $M_H(R_{\max})/M_D$ equals roughly 3.0 ± 1.0.

Thus we may conclude that our numerical results which are consistent with global and local stability require that, of the mass within the edge of the disk, as much as 60%–70% is in a dark, unobserved halo (generally our systems are of late type and have small bulges); and of the remaining disk mass, as much as 30% is also not accounted for by known constituents. We certainly still do not have a very satisfactory answer to the question asked by Toomre (1974): "How can it all be stable?" if the answer is that it is stabilized "by large amounts of matter of which we know absolutely nothing except that it is gravitating."

Next, we comment on a parameter that Toomre (1981) has given for prevention of swing amplification. This is a local parameter that is relevant for the possible development of spiral structure. Following Sellwood (1983), we write Toomre's equations (16) and (17) as

$$X = R\kappa^2/2\pi m G\sigma(R) > 3 , \tag{20}$$

where m is the number of arms. Since we have a flat rotation curve, we can rewrite this as

$$QV_{\text{rot}}/\langle V_R^2 \rangle^{1/2} > 3.97 \text{ m} . \tag{21}$$

It is then the same as Toomre's local stability criterion in equation (4) above if in the latter equation $\langle V_R^2 \rangle^{1/2}$ is replaced by $0.22\, V_{\text{rot}}/m$. Comparison of equation (21) with Table 3 shows that the condition is fulfilled in NGC 7184 only for $m = 1$ at the radii where we observed. NGC 7184 has a more complicated spiral pattern than a simple two-armed design, and this is consistent with the fact that equation (21) is not fulfilled from $m \geq 2$.

Actually, it is easy to show that inequality (20) is always verified only for $m = 1$ as long as $Y \gtrsim 1.1$ (see also Fig. 16 in Sellwood 1983). A straightforward way of illustrating this is to note that for our exponential disk and a flat rotation curve we can write

$$Y = 0.615[QRV_{\text{rot}}/h\langle V_R^2 \rangle^{1/2}]^{1/2} \exp(-R/2h) \tag{22}$$

(see also Efstathiou, Lake, and Negroponte 1982). Since $R/h \exp(-R/h) \leq 0.368$, it easily follows that for $Y \gtrsim 1.1$, equation (20) can be converted into

$$Y^2 \gtrsim \frac{3}{2} m \frac{R}{h} \exp\left(\frac{-R}{h}\right) \gtrsim 0.552m \tag{23}$$

or

$$QV/\langle V_R^2 \rangle^{1/2} \gtrsim 7.91 . \tag{24}$$

So we see from comparing formula (24) to equation (21) that the condition $Y \gtrsim 1.1$ implies that swing amplification is pos-

sible for all modes with $m \geq 2$ at all radii where the rotation curve is flat.

In this paper we have presented data that show the feasibility of observing the stellar kinematics of old disk populations in spiral galaxies. We have for the first time collected data on the radial dependence of both the vertical and radial velocity dispersion in these populations in any spiral galaxy. We summarize our results as follows:

1. In the face-on spiral galaxy NGC 5247, the velocity dispersion in the z-direction of the old disk population decreases with radius. We observe this property out to about 2 scale lengths from the center, and the decrease is consistent with that expected on the basis of a constant M/L in this population in the case observed in edge-on galaxies that the vertical scale parameter is independent of galactocentric distance.

2. The numerical value of the M/L in the *old disk population* is now based on measurements in five galaxies (NGC 891, the Galaxy, NGC 628, 1566, and 5247) and is in the range 6 ± 2 $M_{\odot}/L_{\odot,B}$, where a distance scale based on $H = 75$ km s^{-1} Mpc^{-1} is used.

3. The disks in two samples of galaxies contain, on the basis of this $(M/L)_{\text{old disk}}$, about one-third of the total mass out to the edge of the disk. According to a criterion by Efstathiou, Lake, and Negroponte (1982), this suggests that these disks are stable to global, barlike modes.

4. The radial velocity dispersion also decreases with radius in the disk of NGC 7184. The dependence is similar to that in the vertical velocity dispersion.

5. These dispersions are larger by a factor of ~ 2 than the minimum value given by Toomre (1964) as necessary to suppress local axisymmetric Jeans instabilities. This is in agreement with recent numerical experiments in the literature in which the model disks evolve to comparable equilibrium situations.

We thank the staff of the Anglo-Australian Observatory for their support that made our observing possible. We also acknowledge very useful remarks on an early draft of this paper by Dr. J. A. Sellwood. P.C.K. thanks Mount Stromlo Observatory for hospitality, the Australian National University Research School of Physical Sciences for a grant as visiting fellow to make this visit possible, and Groningen University for granting a leave of absence during the academic year 1982–1983.

REFERENCES

Bahcall, J. N. 1984*a*, *Ap. J.*, **276**, 156.
———. 1984*b*, *Ap. J.*, **276**, 169.
Bahcall, J. N., and Casertano, S. 1984, *Ap, J. (Letters)*, **284**, L35.
Chandrasekhar, S. 1961, *Hydrodynamic and Hydromagnetic Stability* (Oxford: Oxford University Press).
Efstathiou, G., Lake, G., and Negroponte, J. 1982, *M.N.R.A.S.*, **199**, 1069.
Erickson, R. R. 1975, *Ap. J.*, **195**, 343.
Fisher, J. R., and Tully, R. B. 1981, *Ap. J., Suppl.*, **47**, 139.
Gilmore, G., and Reid, N. 1983, *M.N.R.A.S.*, **202**, 1025.
Goldreich, P., and Lynden-Bell, D. 1965, *M.N.R.A.S.*, **130**, 125.
Hoskin, M. A. 1977, *J. Hist. Astr.*, **8**, 77.
Illingworth, G., and Freeman, K. C. 1974, *Ap. J. (Letters)*, **188**, L83.
Jahreiss, H., and Wielen, R. 1983, *IAU Colloquium 76, The Nearby Stars and the Stellar Luminosity Function*, ed., A. G. Davis Philip and A. R. Upgren (Schenectady: Davis), p. 277.
Jeans, J. H. 1928, *Astronomy and Cosmology* (Cambridge: Cambridge University Press).
Kormendy, J. 1984*a*, *Ap. J.*, **286**, 116.
———. 1984*b*, *Ap. J.*, **286**, 132.
Larson, R. B., and Tinsley, B. M. 1978, *Ap. J.*, **219**, 46.
Longo, G., and de Vaucouleurs, A. 1983, *A General Catalogue of Photoelectric Magnitudes and Colors in the U, B, V system of 3,578 Galaxies Brighter than the 16th Magnitude (1936–1982)* (University of Texas Monographs in Astronomy, No. 3).
Mayor, M. 1974, *Astr. Ap.*, **32**, 321.
Oort, J. H. 1965, in *Stars and Stellar Systems*, Vol. **2**, *Galactic Structure*, ed. A. Blaauw, and M. Schmidt (Chicago: University of Chicago Press), p. 455.
Ostriker, J. P., and Peebles, P. J. E. 1973, *Ap. J.*, **186**, 467.
Sandage, A. R., and Tammann, G. A. 1981, *A Revised Shapley-Ames Catalogue* (Washington: Carnegie Institution).
Sargent, W. L. W., Schechter, P. C., Boksenberg, A., and Shortridge, K. 1977, *Ap. J.*, **212**, 326.
Searle, L., Sargent, W. L. W., and Bagnuolo, W. G. 1973, *Ap. J.*, **179**, 427.
Sellwood, J. A. 1983, *I.A.U. Symposium 100, Internal Kinematics and Dynamics of Galaxies*, ed. E. Athanossoula (Dordrecht: Reidel), p. 197.
Sellwood, J. A., and Carlberg, R. G. 1984, *Ap. J.*, **282**, 61.
Shostak, G. S. 1978, *Astr. Ap.*, **68**, 321.
Shostak, G. S., and van der Kruit, P. C. 1984, *Astr. Ap.*, **132**, 20.
Tonry, J., and Davis, M. 1979, *A.J.*, **84**, 1511.
Toomre, A. 1964, *Ap. J.*, **139**, 1217.
———. 1974, *Highlights Astr.*, **3**, 457.
———. 1981, in *Normal Galaxies*, ed. S. M. Fall and D. Lynden-Bell (Cambridge: Cambridge University Press), p. 111.
van der Kruit, P. C. 1979, *Astr. Ap. Suppl.*, **38**, 15.
———. 1981, *Astr. Ap.*, **99**, 298.
———. 1983, *Proc. Astr. Soc. Australia*, **5**, 136.
van der Kruit, P. C., and Freeman, K. C. 1984, *Ap. J.*, **278**, 81.
van der Kruit, P. C., and Searle, L. 1981*a*, *Astr. Ap.*, **95**, 105.
———. 1981*b*, *Astr. Ap.*, **95**, 116.
———. 1982, *Astr. Ap.*, **110**, 61.
van der Kruit, P. C., and Shostak, G. S. 1984, *Astr. Ap.*, **134**, 258.
Wevers, B. M. H. R. 1984, Ph.D. thesis, Rijks Universiteit te Groningen.

K. C. FREEMAN: Mount Stromlo and Siding Spring Observatories, Private Bag, Woden P.O., A.C.T. 2606, Australia

P. C. VAN DER KRUIT: Kapteyn Astronomical Institute, P.O. Box 800, 9700 AV Groningen, The Netherlands